

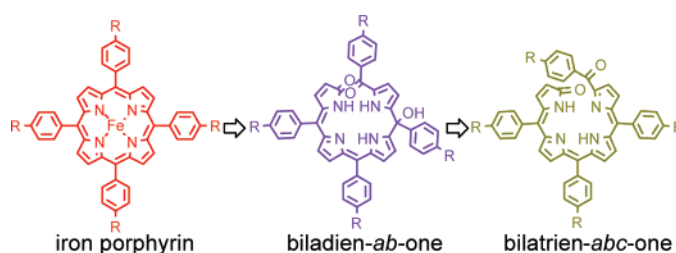
## Synthesis of Biladienone and Bilatrienone by Coupled Oxidation of Tetraarylporphyrins<sup>†</sup>

Naomi Asano, Sayo Uemura, Tomoya Kinugawa, Hiroaki Akasaka, and Tadashi Mizutani\*

Department of Molecular Science and Technology, Faculty of Engineering, Doshisha University,  
Tatara-Miyakotani, Kyotanabe, Kyoto 610-0321, Japan

tmizutan@mail.doshisha.ac.jp

Received April 6, 2007



Tetraarylbiladien-*ab*-ones bearing various substituents (R) in the para position of the phenyl groups were prepared by coupled oxidation of tetraarylporphyrin iron complexes. The yields of 5,10,15-triaryl-19-aro-yl-15-hydroxybiladien-*ab*-ones were 74% (R = H), 85% (R = OMe), 44% (R = COOMe), and 28% (R = CN). Kinetic studies of the iron porphyrin oxidation revealed that the reaction is accelerated by an electron-withdrawing substituent with the Hammett reaction constant  $\rho = 0.295$ . 5,10,15-Triaryl-19-aro-yl-15-hydroxybiladien-*ab*-ones undergo the acid-catalyzed elimination reaction either by acetic acid or by mesoporous silica to afford 5,10,15-triaryl-19-aro-ylbilatrien-*abc*-one. The elimination reaction in acetic acid is accelerated by an electron-donating substituent with the Hammett reaction constant  $\rho = -1.48$ .

### Introduction

Linear tetrapyrroles<sup>1</sup> attract interest owing to their extended  $\pi$ -electron delocalization on a flexible molecular framework, which leads to unique functions as a scaffold of the supramolecular structures<sup>2</sup> as well as molecular electronic materials.<sup>3</sup> As electronic materials, tuning of the HOMO and LUMO levels with appropriate substituents is an attractive strategy, and facile synthesis of various biladienones should be developed for the

application of these compounds. Introduction of appropriate substituents to an aromatic core is also an important strategy for regulation of molecular ordering in crystals or liquid crystals, which greatly affects its performance as a molecular electronic device.<sup>4</sup> Biladienones were prepared from porphyrin via various routes including photochemical oxidation,<sup>5</sup> chemical oxidation,<sup>6</sup> and coupled oxidation.<sup>7</sup> Coupled oxidation of iron porphyrins, oxidation with dioxygen in the presence of a reducing agent such as ascorbic acid in pyridine, was studied by Lemberg<sup>8</sup> in detail. The reaction is called coupled oxidation because oxidation

<sup>†</sup> Dedicated to the memory of Professor Yoshihiko Ito (1937–2006).

\* Author to whom correspondence should be addressed. Phone: 81-774-65-6623. Fax: 81-774-65-6794.

(1) Falk, H. *The Chemistry of Linear Oligoporphyrins and Bile Pigments*; Springer-Verlag: Vienna, New York 1989.

(2) (a) Mizutani, T.; Yagi, S.; Honmaru, A.; Ogoshi, H. *J. Am. Chem. Soc.* **1996**, *118*, 5318. (b) Mizutani, T.; Yagi, S.; Honmaru, A.; Murakami, S.; Furusyo, M.; Takagishi, T.; Ogoshi, H. *J. Org. Chem.* **1998**, *63*, 8769. (c) Mizutani, T.; Yagi, S.; Honmaru, A.; Goldacker, T.; Kitagawa, S.; Furusyo, M.; Takagishi, T.; Ogoshi, H. *Supramol. Chem.* **1999**, *10*, 297. (d) Mizutani, T.; Sakai, N.; Yagi, S.; Takagishi, T.; Kitagawa, S.; Ogoshi, H. *J. Am. Chem. Soc.* **2000**, *122*, 748. (e) Mizutani, T.; Yagi, S. *J. Porphyrins Phthalocyanines* **2004**, *8*, 226. (f) Hamakubo, K.; Yagi, S.; Hama, S.; Nakazumi, H.; Mizutani, T. *Chem. Lett.* **2005**, *34*, 1454.

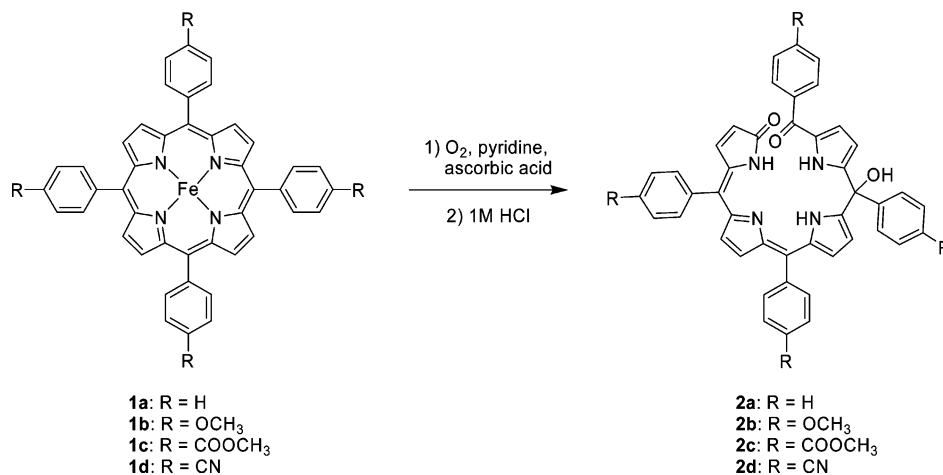
(3) Matsui, E.; Matsuzawa, N. N.; Harnack, O.; Yamauchi, T.; Hatazawa, T.; Yasuda, A.; Mizutani, T. *Adv. Mater.* **2006**, *18*, 2523.

(4) Anthony, J. E.; Brooks, J. S.; Eaton, D. L.; Parkin, S. R. *J. Am. Chem. Soc.* **2001**, *123*, 9482.

(5) (a) Cavaleiro, J. A. S.; Neves, M. G. P. S.; Hewlins, M. J. E.; Jackson, A. H. *J. Chem. Soc., Perkin Trans. 1* **1990**, 1937. (b) Cavaleiro, J. A. S.; Hewlins, M. J. E.; Jackson, A. H.; Neves, M. G. P. M. S. *Tetrahedron Lett.* **1992**, *33*, 6871. (c) Silva, A. M. S.; Neves, M. G. P. M. S.; Martins, R. R. L.; Cavaleiro, J. A. S.; Boschi, T.; Tagliatesta, P. *J. Porphyrins Phthalocyanines* **1998**, *2*, 45. (d) Jeandon, C.; Krattinger, B.; Ruppert, R.; Callot, H. *J. Inorg. Chem.* **2001**, *40*, 3149. (e) Bonnett, R.; Martinez, G. *Tetrahedron* **2001**, *57*, 9513.

(6) (a) Evans, B.; Smith, K. M.; Cavaleiro, J. A. S. *J. Chem. Soc., Perkin Trans. 1* **1978**, 768. (b) Ongayi, O.; Vicente, M. G. H.; Ou, Z.; Kadish, K. M.; Kumar, M. R.; Fronczek, F. R.; Smith, K. M. *Inorg. Chem.* **2006**, *45*, 1463.

## SCHEME 1. Coupled Oxidation of Tetraarylporphyrins



of iron porphyrin occurs only if ascorbic acid is concurrently oxidized. The mechanism of the coupled oxidation has been studied in relation to the heme oxygenase enzymatic reactions. Ortiz de Montellano and co-workers reported that heme oxygenase oxidized porphyrin derivatives carrying a methyl group or a formyl group at the meso position.<sup>9</sup> For the iron porphyrin bearing one methyl group at the meso position, both the methyl group and the meso carbon were eliminated to yield bilindione.<sup>9a</sup> For the iron porphyrin bearing one formyl group at the meso position, the non-formyl-substituted meso carbon was selectively eliminated, demonstrating that electronic effects of the substituent directed the oxidation selectivity.<sup>9b</sup> Although meso-substituted porphyrins were employed as a substrate for the enzyme reactions, the substrate of the coupled oxidation has been limited to the iron complexes of meso-unsubstituted porphyrins such as protoporphyrin IX and octaethylporphyrin. Recently, Niemezv et al. reported that *meso*-monophenylporphyrin underwent coupled oxidation where the meso-unsubstituted carbon was selectively oxidized.<sup>10</sup>

We recently reported that the iron complex of tetraphenylporphyrin also underwent coupled oxidation under mild reaction conditions.<sup>11</sup> In the coupled oxidation of the iron complex of tetraphenylporphyrin, two products with different oxidation levels were obtained, 15-hydroxybiladien-*ab*-one where the meso carbon was retained as the benzoyl carbonyl carbon, and bilindione where a meso carbon and a phenyl group were eliminated. The reaction affording the latter product was

sluggish, and the isolation of the product was laborious. In this paper, we report our efforts to optimize the reaction conditions of coupled oxidation to obtain the former product, 5,10,15-triaryl-19-aroil-15-hydroxybiladien-*ab*-ones with various substituents. We also report that 5,10,15-triaryl-19-aroil-15-hydroxybiladien-*ab*-one undergoes acid-catalyzed thermal elimination reactions to yield a fully  $\pi$ -conjugated bilatrien-*abc*-one.

## Results and Discussion

**Coupled Oxidation of Tetraarylporphyrins.** Coupled oxidation of tetraarylporphyrin proceeds in two steps to yield 5-, 10,15-triaryl-19-aroil-15-hydroxybiladien-*ab*-one and triaryl-bilindione.<sup>11</sup> In the first step, [tetraarylporphyrinato]iron(III) chloride was treated with pyridine, ascorbic acid, and dioxygen in chloroform, and then rapid bleaching of the porphyrin Soret absorption band occurs. In the second step, the resultant reaction mixture was treated with acid to yield violet pigments, biladienones (Scheme 1). Although several products were obtained in the reaction, we optimized the reaction conditions to obtain biladien-*ab*-one **2** selectively.

Figure 1 shows the UV–visible spectral changes of a solution of [5,10,15,20-tetraphenylporphyrinato]iron(III) chloride,

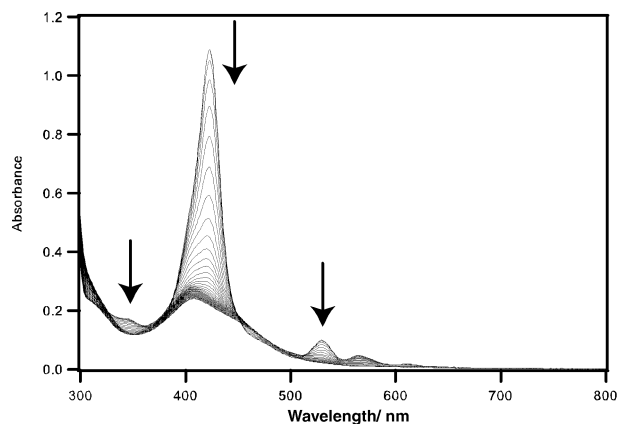


**FIGURE 1.** UV–visible spectral changes of  $1.5 \times 10^{-5}$  M of [5,10,15,20-tetraphenylporphyrinato]iron(II), 1.32 M of pyridine, and  $5.7 \times 10^{-3}$  M of ascorbic acid in dioxygen-saturated chloroform at 25 °C. Spectra were recorded every 1 min, and the half-life was estimated to be 6 min.

(7) (a) Bonnett, R.; Dimsdale, M. J. *Tetrahedron Lett.* **1968**, *9*, 731. (b) Bonnett, R.; Dimsdale, M. J. *J. Chem. Soc., Perkin Trans. 1* **1972**, 2540. (c) Bonnett, R.; McDonagh, A. F. *J. Chem. Soc., Perkin Trans. 1* **1973**, 881. (d) Balch, A. L.; Latos-Grazynski, L.; Noll, B. C.; Olmstead, M. M.; Sztrenberg, L.; Safari, N. *J. Am. Chem. Soc.* **1993**, *115*, 1422. (e) Balch, A. L.; Latos-Grazynski, L.; Noll, B. C.; Olmstead, M. M.; Safari, N. *J. Am. Chem. Soc.* **1993**, *115*, 9056. (f) Morishima, I.; Fujii, H.; Shiro, Y.; Sano, S. *Inorg. Chem.* **1995**, *34*, 1528. (g) Johnson, J. A.; Olmstead, M. M.; Balch, A. L. *Inorg. Chem.* **1999**, *38*, 5379.

(8) (a) Lemberg, R. *Biochem. J.* **1935**, *29*, 1322. (b) Lemberg, R.; Cortis-Jones, B.; Norrie, M. *Biochem. J.* **1938**, *32*, 149.

(9) (a) Torpey, J.; Ortiz, de Montellano, P. R. *J. Biol. Chem.* **1996**, *271*, 26067. (b) Torpey, J.; Ortiz, de Montellano, P. R. *J. Biol. Chem.* **1997**, *272*, 22008.

(10) (a) Niemezv, F.; Alvarez, D. E.; Buldain, G. Y. *Heterocycles* **2002**, *57*, 697. (b) Niemezv, F.; Buldain, G. Y. *J. Porphyrins Phthalocyanines* **2004**, *8*, 989.

(11) Yamauchi, T.; Mizutani, T.; Wada, K.; Horii, S.; Furukawa, H.; Masaoka, S.; Chang, H.-C.; Kitagawa, S. *Chem. Commun.* **2005**, 1309.

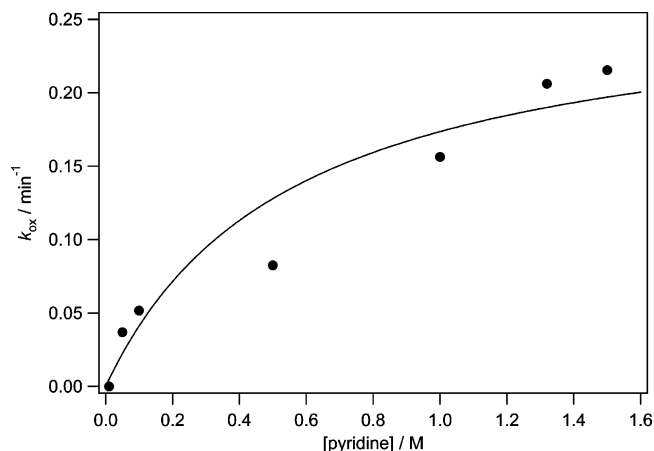


**FIGURE 2.** Plot of the rate constant of the Soret band bleaching of **1a** against pyridine concentration. For the reaction conditions, see the legend to Figure 1.

**TABLE 1.** Rate Constants ( $k_{ox}$ ) of Coupled Oxidation of Iron Porphyrins (298 K,  $\text{CHCl}_3$ )<sup>a</sup>

	substituent	$k_{ox}/\text{min}^{-1}$	$\sigma_p$
<b>1a</b>	H	$0.175 \pm 0.014$	0
<b>1b</b>	OMe	$0.163 \pm 0.017$	-0.27
<b>1c</b>	COOMe	$0.220 \pm 0.022$	0.31
<b>1d</b>	CN	$0.302 \pm 0.020$	0.66

<sup>a</sup> Each rate constant is the average of 3–4 independent determinations.

ascorbic acid, and pyridine in dioxygen-saturated chloroform. The rate of bleaching was first order in the porphyrin concentration.

$$-\frac{d[\mathbf{1}]}{dt} = k_{ox} \quad (1)$$

The first-order rate constant  $k_{ox}$  was determined by following the absorbance changes over one half-life. The rate constants are plotted against the concentration of pyridine in Figure 2. The rate was accelerated by adding pyridine and showed saturation at a high concentration of pyridine (1.3 M).<sup>8a,12</sup> Using 1.3 M of pyridine, several tetraarylporphyrins **1a–d** were subjected to the coupled oxidation. The rate constants of the Soret band bleaching  $k_{ox}$  were determined at 298 K for four iron porphyrins **1a–d** bearing either electron-donating or electron-withdrawing groups and are listed in Table 1. The Hammett plot is shown in Figure 3. Electron-withdrawing substituents accelerated bleaching, and the slope of the line gave the Hammett reaction constant  $\rho$  of 0.295.

For electronic effects on porphyrin oxidation, Torpey and Ortiz de Montellano demonstrated that the oxidation of heme by heme oxygenase occurs via electrophilic attack of oxygen to the meso carbon.<sup>9</sup> We previously reported that coupled oxidation of 18-trifluoromethylporphyrin occurs at the meso-carbon with the highest electron density, C-5, consistent with the mechanism of electrophilic attack of oxygen to the meso carbon.<sup>13</sup> Zhu and Silvermann recently reported that the porphyrin meso positions that are at higher  $\pi$ -electron densities in

(12) For the role of pyridine in the coupled oxidation process of meso-unsubstituted porphyrins, see ref. 8a and Balch, A. L.; Koerner, R.; Latos-Grazynski, L.; Lewis, J. E.; St. Claire, T. N.; Zovinka, E. P. *Inorg. Chem.* **1997**, *36*, 3892.

(13) Crusats, J.; Suzuki, A.; Mizutani, T.; Ogoshi, H. *J. Org. Chem.* **1998**, *63*, 602.

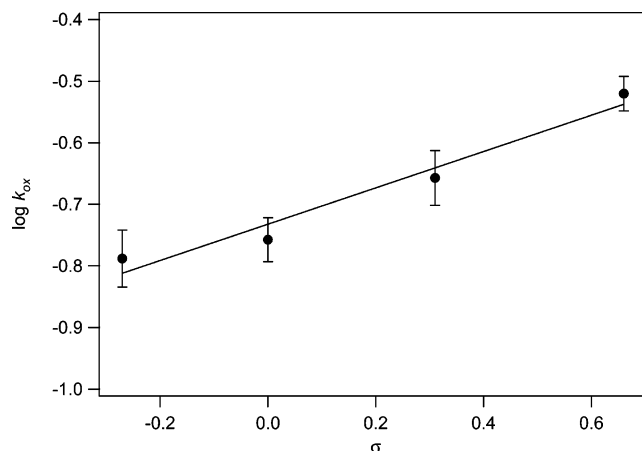


**FIGURE 3.** Plot of the coupled oxidation rate constant against Hammett substituent constant  $\sigma$ . The slope gave the reaction constant  $\rho$  0.295.

ferric 2,4-diacetyldeuteroporphyrin are selectively attacked in the coupled oxidation.<sup>14</sup> These studies revealed that higher  $\pi$ -electron density is favorable for the porphyrin oxidation. If this effect is dominant, we expect that electron-donating substituent in the porphyrin phenyl groups will accelerate the coupled oxidation reaction. Another factor is activation of the coordinated dioxygen by electron-withdrawing substituents. In cytochrome P-450 model reactions, oxidation of cyclohexane with iron porphyrins carrying electron-withdrawing substituents in the phenyl groups proceeds faster than those with electron-donating substituents.<sup>15</sup> The Hammett reaction constant was in the range of 0.3–0.5. Although the intermediate of the P-450 model reaction is different from that of the coupled oxidation, similar activation by electron-withdrawing groups is expected for coupled oxidation. The overall reaction rate will be determined by the balance of these two factors, and the latter factor seems to be dominant in the present reactions.

When bleached solutions were treated with acid, the color of the solution turned violet to yield 15-hydroxybiladien-*ab*-one. Previously we used  $\text{NaBF}_4$  to precipitate the product followed by the acid treatment, but direct treatment of a chloroform solution with 1 M aqueous HCl in a two-phase system is a simple and better procedure to avoid further decomposition of 15-hydroxybiladien-*ab*-one. We reported the longer reaction period for the coupled oxidation of **1d**, but we found that a longer reaction period induced decomposition of the product. The yields of **2a**, **2b**, **2c**, and **2d** were 74, 85, 44, and 28%, respectively. With the reported procedure, the isolated yield of biladien-*ab*-one bearing electron-withdrawing substituents were lower.<sup>11</sup> This is true for the modified procedure reported here. The lower yield of cyanophenyl biladienone **2d** was attributed to the higher reactivity of the porphyrin **1d** toward oxidation. It seems to be more difficult to find out the optimum reaction conditions for the highly reactive iron porphyrin having electron-withdrawing groups.<sup>16</sup>

**Dehydration of 15-Hydroxybiladien-*ab*-one.** The UV–visible spectral changes in a solution of 15-hydroxybiladien-*ab*-ones **2a–d** in acetic acid heated at 45 °C are shown in Figure

(14) Zhu, Y.; Silverman, R. B. *Org. Lett.* **2007**, *9*, 1195.

(15) Guo, C.-C.; Song, J.-X.; Chen, X.-B.; Jiang, G.-F. *J. Mol. Catal. A* **2000**, *157*, 31.

(16) For the oxidation of bile pigments, see Eivazi, F.; Hudson, M. F.; Smith, K. M. *Tetrahedron Lett.* **1976**, 3837.

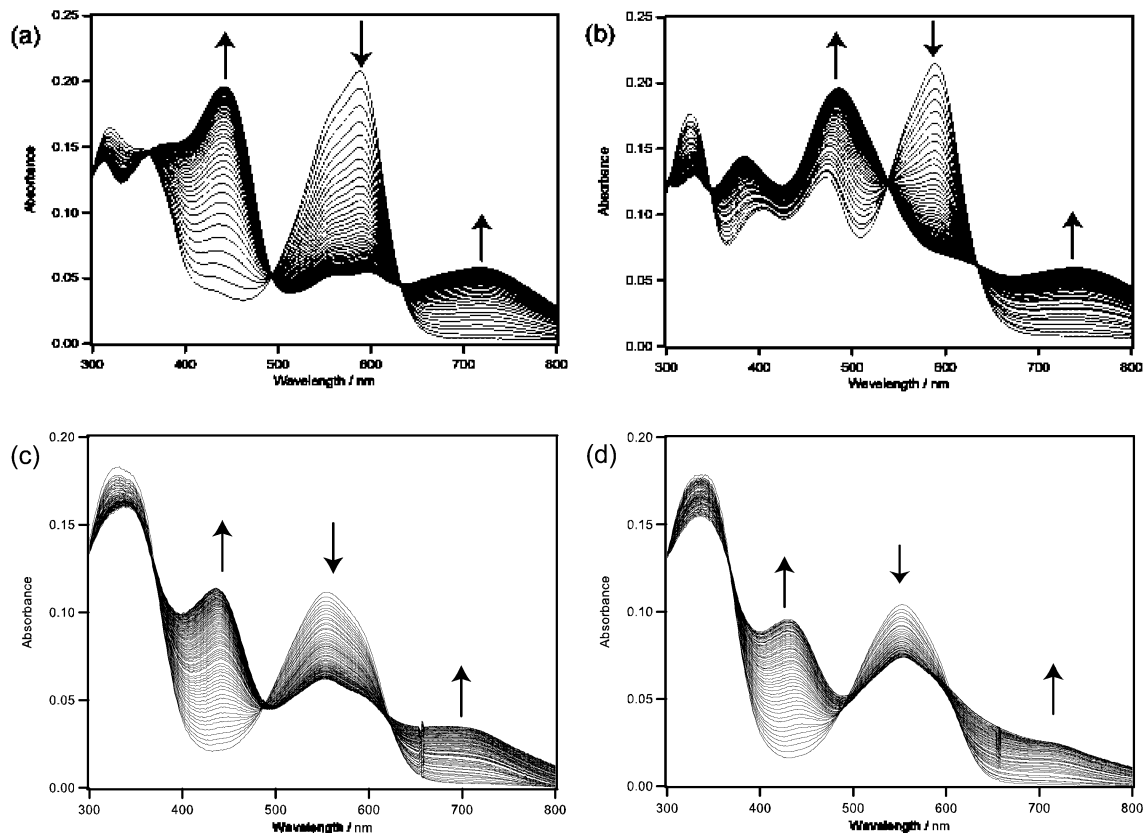


**FIGURE 4.** UV–visible spectral change of **2a** (a), **2b** (b), **2c** (c), and **2d** (d) ( $5 \times 10^{-6}$  M) in acetic acid upon heating (318 K). Spectra were recorded every 1 min (a), 0.5 min (b), 2 min (c), and 10 min (d).

4. For **2a**, the absorbance at 589 nm decreased with concomitant increase in absorbance at 442 and 718 nm. These spectral changes are similar to those observed when the zinc complex of 15-hydroxybiladien-*ab*-one was heated in chloroform to produce the dehydrated bilatrien-*abc*-one zinc complex.<sup>5b</sup> Evaporation of the acetic acid and the residue was analyzed by <sup>1</sup>H NMR. The <sup>1</sup>H NMR spectrum was consistent with the dehydrated bilatrien-*abc*-one structure **3a**.<sup>17</sup> Attempt to isolate pure **3a** was not successful since partial decomposition of **3a** occurs during evaporation of the acetic acid. We found that by using mesoporous silica FSM-16,<sup>18</sup> a solid acid, instead of acetic acid isolation of the product is easier. Thus a solution of biladien-*ab*-one **2a** in benzene was refluxed for 3 h over FSM-16, followed by filtration to remove the catalyst. Evaporation of the benzene gave almost pure **3a**. Apparently FSM-16 acts as a solid acid and a dehydrating agent. Silica gel can also be used as a catalyst, showing similar catalytic activity.

<sup>1</sup>H NMR of **3a** showed that the three NH signals at 10.0, 10.8, and 12.5 ppm of **2a** disappeared and two sets of NH protons appeared at 10.3 and 13.1 ppm (major isomer) and 11.1 and 13.2 ppm (minor isomer), suggesting that two isomers are formed and are in equilibrium. The molar ratio of the major isomer to the minor isomer was ca. 4:1. <sup>13</sup>C NMR showed that the signals at 77 (C-15), 173 (C-1), and 184.7 (C-20, the carbonyl carbon of the 19-benzoyl group) ppm of the starting

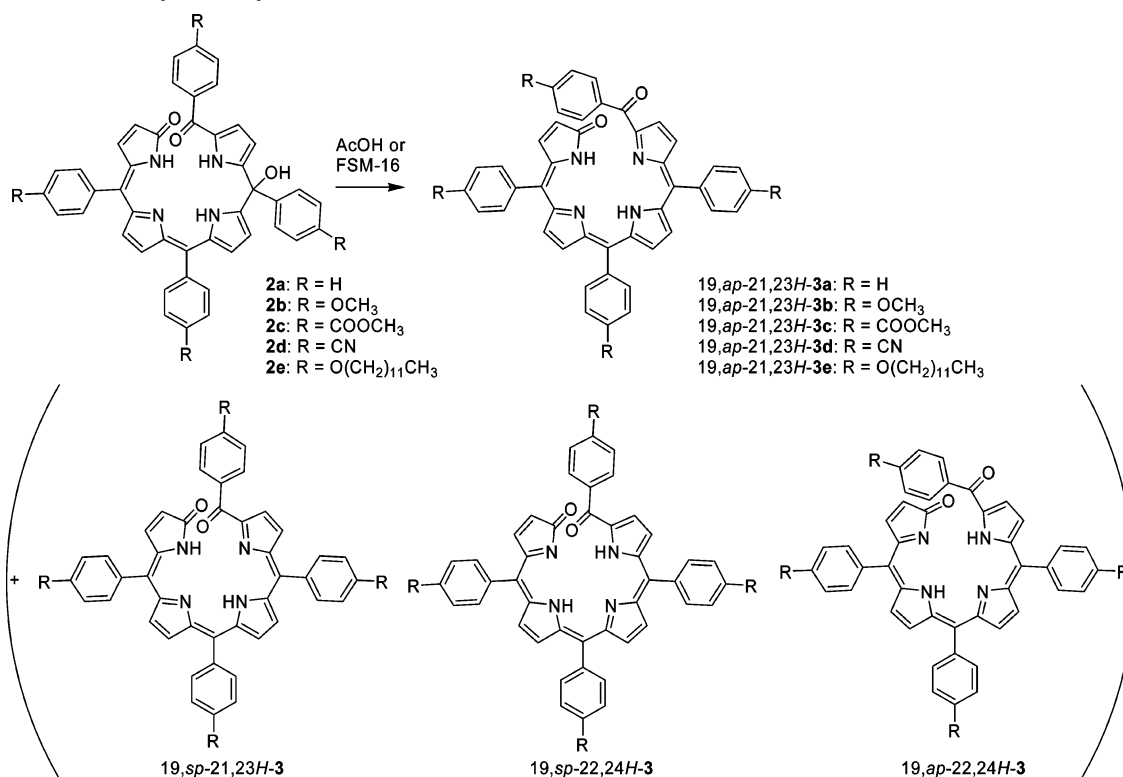
material **2a** disappeared and new signals appeared at 171 and 189 ppm. Since the major and minor isomers showed different <sup>1</sup>H NMR chemical shifts, complete assignment of signals of both isomers were not performed. Instead, the <sup>1</sup>H NMR of the major isomer of (4*Z*,9*Z*,14*Z*)-1,21-dihydro-19-(4-undecyloxybenzoyl)-5,10,15-tris(4-undecyloxyphenyl)-23*H*-bilin-1-one (**3e**)<sup>19</sup> was assigned by <sup>1</sup>H–<sup>1</sup>H COSY, ROESY, and HMBC spectra since <sup>1</sup>H NMR signals of **3e** were better resolved. The HMBC spectrum indicated that there are correlations between C1 and H2/H3, C20 and the ortho proton of the *p*-alkoxybenzoyl group, C19 and H18/H17, and C6 and H7/H8. ROESY correlations were observed between H3 and the ortho protons of the 5-phenyl group, H12 and the ortho protons of the 10-phenyl group, and H17 and the ortho protons of the 15-phenyl group. COSY correlations between NH protons and H2/H3 and H12/H13

(19) Kita, K.; Tokuoka, T.; Monno, E.; Yagi, S.; Nakazumi, H.; Mizutani, T. *Tetrahedron Lett.* **2006**, *47*, 1533.

(20) Frisch, M. J.; Trucks, G. W.; Schlegel, H. B.; Scuseria, G. E.; Robb, M. A.; Cheeseman, J. R.; J. A. Montgomery, J.; Vreven, T.; Kudin, K. N.; Burant, J. C.; Millam, J. M.; Iyengar, S. S.; Tomasi, J.; Barone, V.; Mennucci, B.; Cossi, M.; Scalmani, G.; Rega, N.; Petersson, G. A.; Nakatsuji, H.; Hada, M.; Ehara, M.; Toyota, K.; Fukuda, R.; Hasegawa, J.; Ishida, M.; Nakajima, T.; Honda, Y.; Kitao, O.; Nakai, H.; Klene, M.; Li, X.; Knox, J. E.; Hratchian, H. P.; Cross, J. B.; Adamo, C.; Jaramillo, J.; Gomperts, R.; Stratmann, R. E.; Yazyev, O.; Austin, A. J.; Cammi, R.; Pomelli, C.; Ochterski, J. W.; Ayala, P. Y.; Morokuma, K.; Voth, G. A.; Salvador, P.; Dannenberg, J. J.; Zakrzewski, V. G.; Dapprich, S.; Daniels, A. D.; Strain, M. C.; Farkas, O.; Malick, D. K.; Rabuck, A. D.; Raghavachari, K.; Foresman, J. B.; Ortiz, J. V.; Cui, Q.; Baboul, A. G.; Clifford, S.; Cioslowski, J.; Stefanov, B. B.; Liu, G.; Liashenko, A.; Piskorz, P.; Komaromi, I.; Martin, R. L.; Fox, D. J.; Keith, T.; Al-Laham, M. A.; Peng, C. Y.; Nanayakkara, A.; Challacombe, M.; Gill, P. M. W.; Johnson, B.; Chen, W.; Wong, M. W.; Gonzalez, C.; Pople, J. A.; Gaussian, Inc., Pittsburgh, PA, 2003.

(17) (a) Smith, K. M.; B.; B. S.; Troxler, R. F.; Lai, J.-J. *Tetrahedron Lett.* **1980**, *21*, 2763. (b) Matsuura, T.; Inoue, K.; Ranade, A. C.; Saito, I. *Photochem. Photobiol.* **1980**, *31*, 23.

(18) Inagaki, S.; Fukushima, Y.; Kuroda, K. *J. Chem. Soc., Chem. Commun.* **1993**, 680.

SCHEME 2. Acid-Catalyzed Dehydration of Biladien-*ab*-one 2 To Afford Bilatrien-*abc*-one 3

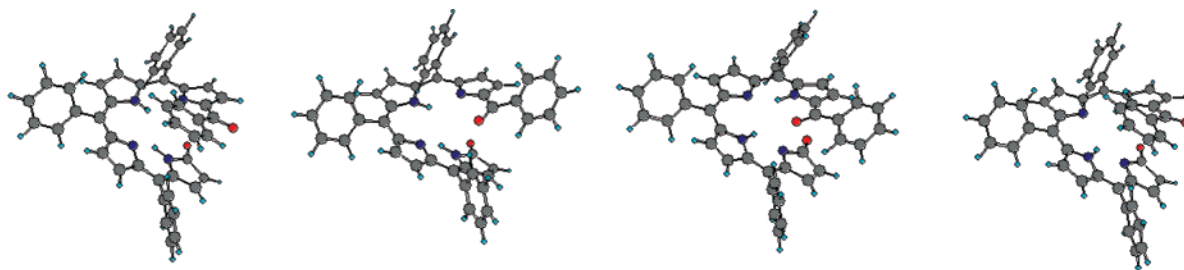
established that the major isomer has protons at N21 and N23. Characteristic feature of the <sup>1</sup>H NMR is that the ortho protons of the 5-phenyl group is shifted upfield. This upfield shift is consistent with the 19-antiperiplanar conformer where the ortho proton of the 5-phenyl group is close to the 20-phenyl group. These spectral features are consistent with the formation of bilatrienone **3e**. For bilatrien-*abc*-one, there are several isomers as shown in Scheme 2, such as the positional isomers of the protonated nitrogens and the synperiplanar/antiperiplanar (*sp/ap*) isomers of the C19–C20 bond. B3LYP/6-31G\* calculations indicate that the 19,*ap*-21,23*H* isomer is the most stable (Figure 5). On the basis of NMR studies, the major isomer was assigned to 19,*ap*-21,23*H*-**3e**. The structure of the minor isomer was not determined: a similar <sup>1</sup>H NMR pattern suggests that the minor isomer has similar structure to that of the major isomer.

The UV–visible spectral changes due to the conversion of **2** to **3** were analyzed based on the first-order kinetics,

and the rate constants  $k_{el}$  of the elimination reaction were determined.

$$-\frac{d[\mathbf{2}]}{dt} = k_{el} \quad (2)$$

The first-order rate constants  $k_{el}$  are listed in Table 2. For **2a** and **2b**, UV–visible spectral changes showed isobestic points while for **2c** and **2d**, no isobestic points were observed. The absence of isobestic points may be due to the formation of isomers as shown in Scheme 2. Plot of  $\log k_{el}$  against  $\sigma$  gave the slope of  $-1.48$  as a Hammett reaction constant (Figure 6). The dehydration is accelerated by electron-donating substituents, and the E1 mechanism where a carbenium ion is an intermediate is proposed. The dihedral angle of the 15-phenyl group and the dipyrromethene in **3a** was  $52.8^\circ$  according to the molecular orbital calculations (B3LYP/6-31G\*). Therefore we suggest that  $\pi$ -electron conjugation between the carbenium ion at C-15 and

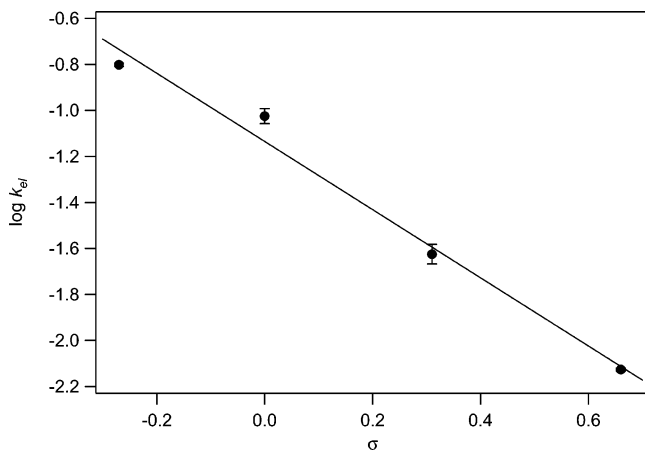


Compounds	19, <i>ap</i> -21,23 <i>H</i> -3	19, <i>sp</i> -21,23 <i>H</i> -3	19, <i>sp</i> -22,24 <i>H</i> -3	19, <i>ap</i> -22,24 <i>H</i> -3
Energy in atomic unit	-2064.1836 au	-2064.1799 au	-2064.1756 au	-2064.1719 au
Relative energy in kcal/mol	0	2.3	5.0	7.3

**FIGURE 5.** Relative energy of four isomers of bilatrien-*abc*-one **3a** geometry optimized by molecular orbital calculations at the B3LYP/6-31G\* level.<sup>20</sup>

**TABLE 2.** Rate Constants of Dehydration of 15-Hydroxybiladien-*ab*-ones (298 K, acetic acid)

	substituent	$k_{\text{el}}/\text{min}^{-1}$	$\sigma_{\text{p}}$
2a	H	$(9.44 \pm 0.70) \times 10^{-2}$	0
2b	OMe	$(1.58 \pm 0.03) \times 10^{-1}$	-0.27
2c	COOMe	$(2.37 \pm 0.23) \times 10^{-2}$	0.31
2d	CN	$(7.48 \pm 0.11) \times 10^{-3}$	0.66

**FIGURE 6.** Plot of the dehydration rate constant  $k_{\text{el}}$  against the Hammett substituent constant. The slope gave the reaction constant  $\rho = -1.48$ . Each rate constant is the average of three to five independent determinations.

the *p*-OMe occurs only partially. Therefore, use of  $\sigma$  instead of  $\sigma^+$  would be more appropriate. Linear correlation was indeed obtained using  $\sigma$ .

In conclusion, 15-hydroxybiladien-*ab*-ones and bilatrien-*abc*-ones with various substituents were prepared by coupled oxidation and the subsequent acid-catalyzed elimination reaction, respectively. Electronic effects of substituents were analyzed by the Hammett equation. Coupled oxidation of the iron tetraarylporphyrin was accelerated by electron-withdrawing substituents while elimination of 15-hydroxybiladien-*ab*-one to bilatrien-*abc*-one was accelerated by electron-donating substituents. The lower isolated yield of the 15-hydroxybiladien-*ab*-one bearing electron-withdrawing substituents was attributed to the higher reactivity of the porphyrin, for which optimization of the reaction conditions was more difficult.

## Experimental Section

**(4Z,9Z)-1,15,21,24-Tetrahydro-19-benzoyl-15-hydroxy-5,10,15-triphenyl-23H-bilin-1-one (2a).** [5,10,15,20-tetraphenylporphyrinato]iron(III) chloride (38 mg, 0.055 mmol) was placed in a 100-mL flask, and 6 mL of pyridine was added. A 50 mL amount of dioxygen-saturated  $\text{CHCl}_3$  was added, followed by 0.51 g (2.85 mmol) of ascorbic acid. The solution was stirred at room temperature with dioxygen bubbling. The reaction mixture was diluted with  $\text{CHCl}_3$  (50 mL), and 1 M HCl (150 mL) was added. The solution was stirred at room temperature for 1 h. The  $\text{CHCl}_3$  layer was separated and washed with water twice. The organic layer was dried over anhydrous sodium sulfate, and the solvent was evaporated in vacuo. The residue was chromatographed on silica ( $\text{CH}_2\text{Cl}_2$ :acetone = 96:4) to afford a violet crystal (28 mg, 73.7%).  $^1\text{H NMR}$  (500 MHz,  $\text{CDCl}_3$ )  $\delta$  6.18 (m, 3H, H-2, 13, 17), 6.32 (d, 1H, H-7), 6.36 (s, 1H, OH), 6.49 (1H, d, H-12), 6.78 (d, 1H, H-8), 6.82 (dd, 1H, H-18), 6.89 (d, 1H, H-3), 7.88 (d, 2H, ortho-H of 20-phenyl), 9.95 (1H, s, 23N-H), 10.8 (1H, s, 21N-H), 12.5 (1H, s, 24N-H). FAB-MS (3-nitrobenzyl alcohol)  $m/z = 647$  ( $\text{M} - \text{OH}^+$ ), 664 ( $\text{M}^+$ ).

**5,10,15,20-Tetrakis(4-methoxyphenyl)porphyrin (TPP-OMe).** To refluxed propionic acid (600 mL) in a 1-L three-necked flask

were added pyrrole (11.2 mL, 0.16 mol) and *p*-methoxybenzaldehyde (19.4 mL, 0.16 mol), and the solution was refluxed for 30 min in dark. After the reaction mixture was cooled to room temperature, crystals were collected by suction-filtration and washed with methanol. The crystals were dissolved in chloroform and reprecipitated with an excess amount of methanol to afford 5.15 g (17.5%) of violet crystals.  $^1\text{H NMR}$  (500 MHz,  $\text{CDCl}_3$ )  $\delta$  8.86 (s, 8H), 8.12 (d, 8H), 7.28 (d, 8H), 4.10 (s, 12H), -2.75 (s, 2H), FAB-MS  $m/z$  734 ( $\text{M}^+$ ).

**[5,10,15,20-Tetrakis(4-methoxyphenyl)porphyrinato]iron(III) Chloride (1b).** TPP-OMe 2.51 g (3.42 mmol) was placed in a 500-mL three-necked flask, DMF (50 mL) was added, and the solution was refluxed.  $\text{FeCl}_2 \cdot 4\text{H}_2\text{O}$  (21.8 g, 0.11 mol) in 200 mL of DMF was then added, and the solution was refluxed for 3 h. After the mixture was cooled to room temperature, 600 mL of  $\text{CHCl}_3$  was added. The organic layer was washed three times with 1 M HCl and twice with water. The organic layer was dried over anhydrous sodium sulfate and evaporated to afford 2.81 g (99.8%) of dark violet crystals. FAB-MS  $m/z$  788 ( $\text{M} - \text{Cl}^-$ ).

**(4Z,9Z)-1,15,21,24-Tetrahydro-19-(4-methoxybenzoyl)-15-hydroxy-5,10,15-tris(4-methoxyphenyl)-23H-bilin-1-one (2b).** [5,10,15,20-Tetrakis(4-methoxyphenyl)porphyrinato]iron(III) chloride (38.1 mg, 0.0484 mmol) was placed in a 100-mL flask, and 6 mL of pyridine was added. A 50 mL amount of dioxygen-saturated  $\text{CHCl}_3$  was added, followed by 0.51 g of L-ascorbic acid. The solution was stirred at room temperature for 1 h with dioxygen bubbling. The reaction mixture was diluted with  $\text{CHCl}_3$  (50 mL), and 1 M HCl (150 mL) was added. The solution was stirred at room temperature for 1 h. The  $\text{CHCl}_3$  layer was separated and washed with water twice. The organic layer was dried over anhydrous sodium sulfate, and the solvent was evaporated in vacuo. The residue was chromatographed on silica ( $\text{CH}_2\text{Cl}_2$ :acetone = 96:4) to afford 32 mg (84.7%) of violet crystals.  $^1\text{H NMR}$  (500 MHz,  $\text{CDCl}_3$ )  $\delta$  3.80 (s, 3H), 3.87 (s, 3H), 3.88 (s, 3H), 3.89 (s, 3H), 6.18 (m, 3H, H-2, 13, 17), 6.38 (d, 1H, H-7), 6.32 (s, 1H, OH), 6.52 (1H, d, H-12), 6.82 (m, 2H, H-8, 18), 6.89 (d, 2H, meta-H of 15-phenyl), 6.90 (d, 1H, H-3), 6.95 (d, 2H, meta-H of 20-phenyl), 6.96 (d, 2H, meta-H of 5-phenyl), 6.98 (d, 2H, meta-H of 10-phenyl), 7.29 (d, 2H, ortho-H of 5-phenyl), 7.39 (d, 2H, ortho-H of 15-phenyl), 7.49 (d, 2H, ortho-H of 10-phenyl), 7.91 (d, 2H, ortho-H of 20-phenyl), 9.90 (s, 1H, 24N-H), 11.0 (s, 1H, 21N-H), 12.3 (s, 1H, 23N-H). FAB-MS (3-nitrobenzyl alcohol)  $m/z = 767$  ( $\text{M} - \text{OH}^+$ ), 784 ( $\text{M}^+$ ).

**5,10,15,20-Tetrakis(4-methoxycarbonylphenyl)porphyrin (TPP-COOMe).** To refluxed propionic acid (150 mL) in a 500-mL three-necked flask were added pyrrole (2.8 mL, 0.04 mol) and methyl *p*-formylbenzoate (6.57 g, 0.04 mol), and the solution was refluxed for 30 min in dark. After the reaction mixture was cooled to room temperature, crystals were collected by suction-filtration to afford 1.25 g (14.8%) of violet crystals.  $^1\text{H NMR}$  (500 MHz,  $\text{CDCl}_3$ )  $\delta$  8.82 (s, 8H), 8.44 (d, 8H), 8.3 (d, 8H), 4.11 (s, 12H), -2.82 (s, 2H), FAB-MS  $m/z$  846 ( $\text{M}^+$ ).

**[5,10,15,20-Tetrakis(4-methoxycarbonylphenyl)porphyrinato]iron(III) Chloride (1c).** A solution of TPP-COOMe 0.504 g (0.59 mmol) and  $\text{FeCl}_2 \cdot 4\text{H}_2\text{O}$  (2.3 g, 11.8 mmol) in 50 mL of DMF was refluxed for 4 h. After the mixture was cooled to room temperature, 300 mL of  $\text{CHCl}_3$  was added. The organic layer was washed three times with 1 M HCl and twice with water. The organic layer was dried over anhydrous sodium sulfate and evaporated to afford 0.485 g (91.2%) of dark violet crystals. FAB-MS  $m/z$  900 ( $\text{M} - \text{Cl}^-$ ).

**(4Z,9Z)-1,15,21,24-Tetrahydro-19-(4-methoxycarbonylbenzoyl)-15-hydroxy-5,10,15-tris(4-methoxycarbonylphenyl)-23H-bilin-1-one (COOMeBD, 2c).** [5,10,15,20-Tetrakis(4-methoxycarbonylphenyl)porphyrinato]iron(III) chloride 38.5 mg (42.8 mmol) was placed in a 100-mL flask, and 6 mL of pyridine was added. 50 mL of dioxygen-saturated  $\text{CHCl}_3$  was added, followed by 0.5 g of L-ascorbic acid. The solution was stirred at room temperature for 1 h with dioxygen bubbling. To the reaction mixture was added 150 mL of 1 M aqueous HCl. The mixture was stirred for 3 h at

room temperature. The organic layer was separated, washed with water twice, dried over anhydrous sodium sulfate, and evaporated. The residue was chromatographed on silica gel column (CHCl<sub>3</sub>: acetone, 96:4) to obtain 17 mg (44.4%) of violet crystals. <sup>1</sup>H NMR (500 MHz, CDCl<sub>3</sub>) δ 3.91 (s, 3H), 3.95 (s, 3H), 3.96 (s, 3H), 3.97 (s, 3H), 6.17 (m, 2H, H-12, 17), 6.23 (d, 1H, H-2), 6.47 (s, 1H, OH), 6.27 (1H, d, H-7), 6.43 (d, 1H, H-13), 6.74 (1, 2H, H-8), 6.80 (dd, 1H, H-18), 6.85 (d, 1H, H-3), 7.44 (d, 2H, ortho-H of 5-phenyl), 7.59 (d, 4H, ortho-H of 10,15-phenyl), 7.90 (d, 2H, ortho-H of 20-phenyl), 8.10 (m, 8H, meta-H of 5,10,15-phenyl), 10.0 (s, 1H, 24N-H), 10.8 (s, 1H, 21N-H), 12.5 (s, 1H, 23N-H). FAB-MS (3-nitrobenzyl alcohol) *m/z* = 879 (M - OH<sup>+</sup>), 896 (M<sup>+</sup>).

**5,10,15,20-Tetrakis(4-cyanophenyl)porphyrin (TPP-CN).** To refluxed propionic acid (60 mL) in a 100-mL three-necked flask were added pyrrole (1.12 mL, 0.016 mol) and *p*-cyanobenzaldehyde (2.1 g, 16 mmol), and the solution was refluxed for 30 min in the dark. After the reaction mixture was cooled to room temperature, crystals were collected by suction-filtration and washed with methanol. The crystal was dissolved in dichloromethane and chromatographed on silica gel (CH<sub>2</sub>Cl<sub>2</sub>) to afford 0.15 g (5.3%) of violet crystals. <sup>1</sup>H NMR (500 MHz, CDCl<sub>3</sub>) δ 8.79 (s, 8H), 8.33 (d, 8H), 8.10 (d, 8H), -2.89 (s, 2H), FAB-MS *m/z* 715 (M+H<sup>+</sup>).

**[5,10,15,20-Tetrakis(4-cyanophenyl)porphyrinato]iron(III) Chloride (FeCl(TPP-CN), 1d).** TPP-CN 103 mg (0.144 mmol) was placed in a 200-mL three-necked flask, and DMF (50 mL) was added and refluxed. FeCl<sub>2</sub>·4H<sub>2</sub>O (0.836 g, 4.2 mmol) in 50 mL of DMF was then added, and the solution was refluxed for 7 h. After the mixture was cooled to room temperature, 200 mL of CH<sub>2</sub>Cl<sub>2</sub> was added. The organic layer was washed three times with 300 mL of 1 M HCl and twice with water. The organic layer was dried over anhydrous sodium sulfate and evaporated to afford 0.104 g (89.7%) of dark violet crystals. FAB-MS *m/z* 768 (M - Cl<sup>-</sup>).

**(4Z,9Z)-1,15,21,24-Tetrahydro-19-(4-cyanobenzoyl)-15-hydroxy-5,10,15-tris(4-cyanophenyl)-23H-bilin-1-one (2d).** [5,10,15,20-Tetrakis(4-cyanophenyl)porphyrinato]iron(III) chloride (**1d**) (18 mg, 0.0234 mmol) was placed in a 100-mL flask, and 3 mL of pyridine was added. A 25 mL amount of dioxygen-saturated CHCl<sub>3</sub> was added, followed by 0.25 g of L-ascorbic acid. The solution was

stirred at room temperature for 1 h with dioxygen bubbling. The reaction mixture was transferred to 300 mL beaker, 50 mL of 1 M aqueous HCl was added, and the mixture was stirred at room temperature for 3 h. The organic layer was separated, washed with water twice, dried over anhydrous sodium sulfate, and evaporated. The residue was chromatographed on silica gel column (CHCl<sub>3</sub>: acetone, 96:4) to obtain 5 mg (28.0%) of violet crystals. <sup>1</sup>H NMR (500 MHz, CDCl<sub>3</sub>) δ 6.16 (dd, 1H, H-17), 6.26 (d, 1H, H-2), 6.28 (d, 1H, H-7), 6.40 (1H, d, H-12), 6.52 (s, 1H, OH), 6.72 (d, 1H, H-8), 6.79 (dd, 1H, H-18), 6.85 (d, 1H, H-3), 7.49 (d, 2H, ortho-H of 5-phenyl), 7.63 (d, 2H, ortho-H of 10-phenyl), 7.64 (d, 2H, ortho-H of 15-phenyl), 7.69 (d, 2H, meta-H of 15-phenyl), 7.78 (m, 4H, meta-H of 5- and 20-phenyl), 7.79 (d, 2H, meta-H of 10-phenyl), 7.94 (d, 2H, ortho-H of 20-phenyl), 10.1 (s, 1H, 24N-H), 10.8 (s, 1H, 21N-H), 12.4 (s, 1H, 23N-H). <sup>13</sup>C NMR (CDCl<sub>3</sub>) δ 183 (C-1), 173 (C-20), 74 (C-15). FAB-MS (3-nitrobenzyl alcohol) *m/z* = 747 (M - OH<sup>+</sup>), 764 (M<sup>+</sup>).

**(4Z,9Z,14Z)-1,21-Dihydro-19-(4-undecyloxybenzoyl)-5,10,15-tris(4-undecyloxyphenyl)-23H-bilin-1-one (3e).** The major isomer was assigned by <sup>1</sup>H-<sup>1</sup>H COSY, ROESY, and HMBC spectra: <sup>1</sup>H NMR (500 MHz, CDCl<sub>3</sub>) δ 0.88 (t, 12H), 1.26-1.49 (m, 72H), 1.73-1.89 (m, 8H), 3.96-4.09 (m, 8H), 6.05 (d, 1H, H-2), 6.45 (d, 1H, H-17), 6.50 (d, 2H, H-3' of 20-aryl), 6.72 (d, 1H, H-13), 6.74 (d, 1H, H-3), 6.79 (d, 1H, H-12), 6.87 (d, 2H, H-2' of 5-aryl), 6.95-6.99 (m, 5H, H-18, H-3' of 5-aryl, H-3' of 15-aryl), 6.99-7.03 (m, 3H, H-8, H-3' of 10-aryl), 7.13 (d, 1H, H-7), 7.50 (d, 2H, H-2' of 15-aryl), 7.59 (d, 2H, H-2' of 10-aryl), 8.18 (d, 2H, H-2' of 20-aryl), 10.08 (br s, 1H, N<sub>21</sub>-H), 13.05 (br s, 1H, N<sub>23</sub>-H).

**Supporting Information Available:** <sup>1</sup>H NMR spectra and <sup>13</sup>C NMR spectra of **2a**, **2b**, **2c**, **2d**, and **3e**. 2D COSY, ROESY/NOESY, and HMBC analysis of **2c**, **2d**, and **3e**. B3LYP/6-31G\*-optimized geometries and Cartesian coordinates and total energy of **19,ap-21,23H-3**, **19,sp-21,23H-3**, **19,sp-22,24H-3**, **19,ap-22,24H-3**. This material is available free of charge via the Internet at <http://pubs.acs.org>.

JO070692A